Available online at www.sciencedirect.com

SciVerse ScienceDirect

Journal of the European Ceramic Society 32 (2012) 1035–1040

www.elsevier.com/locate/jeurceramsoc

Transparent yttria produced by spark plasma sintering at moderate temperature and pressure profiles

Liqiong An [a,b], Akihiko Ito [a,*], Takashi Goto [a]

[a] *Institute for Materials Research, Tohoku University, Sendai 980-8577, Japan*
[b] *Research Fellow of the Japan Society for the Promotion of Science, Japan*

Received 6 October 2011; received in revised form 4 November 2011; accepted 19 November 2011
Available online 14 December 2011

Abstract

Transparent yttria (Y_2O_3) bodies were fabricated by spark plasma sintering, and the effects of the sintering temperature on relative density, microstructure, and the optical and mechanical properties of Y_2O_3 bodies were investigated. Fully dense Y_2O_3 bodies were obtained at sintering temperatures 1473–1873 K. The average grain size was 0.24–0.32 μm at 1473–1573 K, and steadily increased to 1.97 μm with an increase in temperature to 1823 K. The highest transmittance was obtained in the Y_2O_3 body sintered at 1573 K and annealed at 1323 K, showing 81.7% (99% of the theoretical value) at a wavelength of 2000 nm.

Keywords: Y_2O_3; Sintering; Optical property; Grain growth; Spark plasma sintering

1. Introduction

Yttria (Y_2O_3) is a promising material for application in high-power lasers,[1] infrared windows[2] and high-temperature refractories.[3] Since an Y_2O_3 single crystal is difficult to grow owing to its high melting point (2700 K),[4] transparent polycrystalline ceramic obtained by sintering is an alternative for practical applications. Transparent Y_2O_3 ceramic has been fabricated by pressureless sintering in a vacuum[5–7] or in a H_2 atmosphere,[8] hot pressing[9,10] and hot isostatic pressing.[11,12] In these methods, however, the sintering temperatures are high (above 1853 K) and the grain size is large, usually several ten of micrometers in diameter. Large-grained ceramics tend to have low strength, which deteriorates further in practical applications.

Y_2O_3 bodies with a submicrometer grain size have recently been prepared by the hot isostatically pressed two-step sintering method.[13] Spark plasma sintering (SPS) is another candidate for fabrication of transparent ceramics with submicron grains. The distinctive features of the SPS process are fast densification, short holding time and low sintering temperature.[14] An Y_2O_3 body with a relative density of 97% has been prepared by SPS at a low sintering temperature of 1123 K with a heating rate of 0.17 K s^{-1} for 3.6 ks.[15] Chaim et al. reported an Y_2O_3 body with a relative density greater than 98% prepared by SPS at 1673 K and 3 K s^{-1} for 300 s.[16] However, these Y_2O_3 bodies were not transparent because their relative densities were not high enough; it should be greater than 99%. By using either a significantly low heating rate (0.03 K s^{-1})[17] or a high pressure (300 MPa),[18] transparent Y_2O_3 bodies have been obtained by SPS.

In this study, we prepared a highly transparent Y_2O_3 body at moderate temperature and pressure profiles, and investigated the effects of SPS sintering conditions on the microstructure, and the optical and mechanical properties of Y_2O_3 bodies.

2. Experimental procedure

Y_2O_3 powder (purity: 99.999%, Jiahua Corp., China) was used as the starting material. The as-received powder was ball milled in ethanol using zirconia balls for 12 h and dried at 333 K in an oven for 24 h. The powder was ground and sieved through a 200-mesh grid and calcined at 1273 K in air for 7.2 ks in an electric furnace.

* Corresponding author at: 2-1-1 Katahira, Aoba-ku, Sendai 980-8577, Japan. Tel.: +81 22 215 2106; fax: +81 22 215 2107.
E-mail address: itonium@imr.tohoku.ac.jp (A. Ito).

0955-2219/$ – see front matter © 2011 Elsevier Ltd. All rights reserved.
doi:10.1016/j.jeurceramsoc.2011.11.023

The calcined powder was poured into a graphite die with an inner diameter of 10 mm and sintered by SPS (SPS-210 LX, Fuji Electronic Industrial Co., Ltd, former SPS Syntex Inc., Japan) in a vacuum. The temperature of the graphite die surface was measured using a radiation pyrometer. The sintering temperature was increased to 873 K in 180 s and to 1373 K in 300 s, and then held for 300 s. The sintering temperature was further increased to 1373–1823 K at a heating rate of 0.17 K s^{-1} and maintained at that temperature for 2.7 ks. A pressure of 10 MPa was pre-loaded between room temperature and 1373 K and a final pressure of 100 MPa was loaded above 1373 K and maintained until the end of the sintering process. Post-annealing was carried out at 1123–1423 K for 21.6 ks in air. Both sides of the sintered bodies were mirror-polished using a diamond slurry (1 μm).

The specific surface area of the Y_2O_3 powder after calcination was measured by the Brunauer–Emmett–Teller (BET) method using a surface area and pore size analyzer (TriStar 3000, Micromeritics Instruments Corp., USA) with nitrogen (N_2) adsorption at room temperature. The particle size (d_{BET}) was calculated using the following equation:

$$d_{BET} = \frac{6}{\rho \times S_{BET}}, \quad (1)$$

where ρ is the theoretical density of Y_2O_3 (5.031 Mg m^{-3}) and S_{BET} is the specific surface area measured by the BET method. The density of the sintered bodies was measured by the Archimedes method in distilled water. The crystal phase was identified by X-ray diffraction (XRD, RAD-2C, Rigaku Corp., Japan) using graphite monochromatic CuKα radiation (wavelength: 0.154 nm). The polished surfaces of the Y_2O_3 bodies were thermally etched in air for 3.6 ks at 100–200 K below the sintering temperature. The morphology of the Y_2O_3 powders and the microstructure of the sintered bodies were observed by a field emission scanning electron microscope (FESEM, JSM-7500F, JEOL Ltd., Japan) and a scanning electron microscope (SEM, S-3100H, Hitachi Ltd., Japan). The average grain size was determined from the linear intercept length of the thermally etched surfaces using FESEM and SEM micrographs (assuming a grain size 1.56 times the mean intercept) with at least 250 grains counted.[19] In-line transmittance was measured using a spectrophotometer (UV-3101PC, Shimadzu Corp., Japan) in the wavelength between 190 and 2500 nm. The thickness of the specimens was about 1 mm. Vickers hardness (H_V) was measured by a hardness tester (HM-221, Mitutoyo Corp., Japan) at a load (P) of 2.94 N at room temperature. The fracture toughness was calculated by Eq. (1) using the half length of the crack (c) formed around the corners of the indentations:[20]

$$K_{IC} = 0.073 \times \frac{P}{C^{1.5}}. \quad (2)$$

3. Results and discussion

Fig. 1 shows an FESEM image of calcined Y_2O_3 powder. The powder was slightly agglomerated with nearly spherical grains having an average size of about 100 nm. The specific surface area (BET) of the calcined powder was 12.8 m^2 g^{-1}, and the calculated equivalent particle size was 93 nm, which was well in accordance with the result from the FESEM.

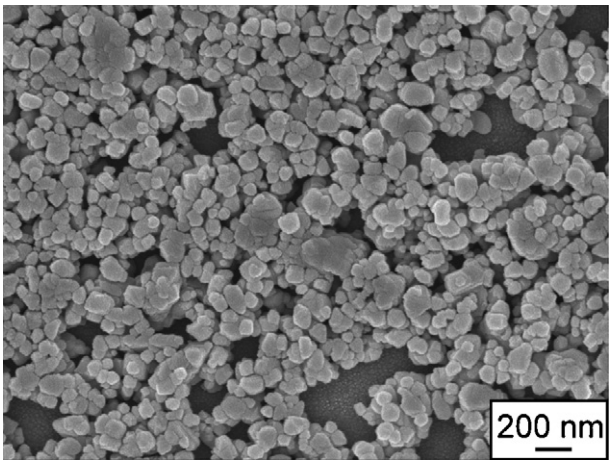

Fig. 1. FESEM image of Y_2O_3 calcined powder.

Fig. 2 shows XRD patterns of calcined Y_2O_3 powder and Y_2O_3 bodies sintered at 1573 K before and after annealing. The patterns were indexed as cubic Y_2O_3 (space group: $Ia\bar{3}$; a = 1.06041 nm; JCPDS no. 41-1105) in all the specimens. Sharp peaks were observed in the sintered Y_2O_3 bodies, *i.e.*, the (2 2 2) peak had a full-width at half-maximum of 0.471° and 0.188° before (Fig. 2a) and after sintering (Fig. 2b and c), respectively. The lattice parameters of Y_2O_3 bodies sintered at 1573 K before (Fig. 2b) and after (Fig. 2c) annealing were 1.06048 (0.00005) and 1.06057 (0.00006) nm, respectively. These were in agreement to the reported value (1.06041 nm).

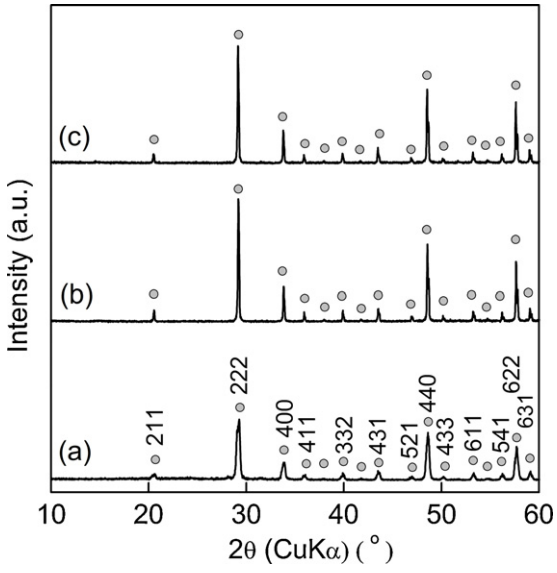

Fig. 2. X-ray diffraction patterns of (a) Y_2O_3 calcined powder, and Y_2O_3 bodies sintered at 1573 K (b) and (c) after annealing at 1323 K for 21.6 ks in air.

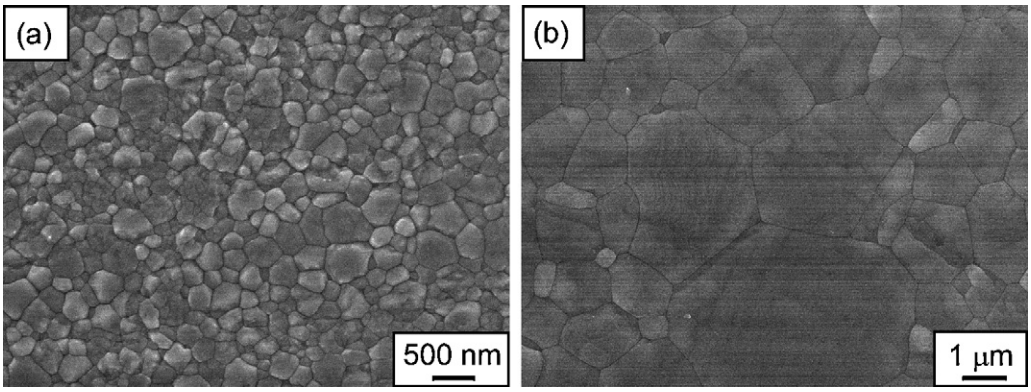

Fig. 3. FESEM images of Y_2O_3 bodies sintered at (a) 1573 K and (b) 1823 K.

Fig. 3 shows FESEM images of Y_2O_3 bodies sintered at 1573 and 1823 K. Pores were rarely observed in either of the specimens. The grains were uniform with an average grain size of 0.32 μm at a sintering temperature of 1573 K (Fig. 3a), whereas they grew to 1.97 μm and the grain size distribution was widened at 1823 K (Fig. 3b). Fig. 4 shows the effect of sintering temperature on the relative density and average grain size of Y_2O_3 bodies sintered at 1373–1823 K. The relative density was 98% of the theoretical value at 1373 K and fully dense bodies (above 99%) were obtained in the temperatures 1473–1823 K. The average grain size slightly increased from 0.24 to 0.32 μm at sintering temperatures 1473–1573 K, and significantly increased to 1.97 μm with an increase in temperature to 1823 K.

Fig. 5 shows FESEM images of the fracture surfaces of Y_2O_3 bodies sintered at 1473–1773 K. The fracture mode was mainly transgranular. Small pores were observed at the triple junction of the grain boundaries and grain interiors in all the specimens (as indicated by open circles in Fig. 5).

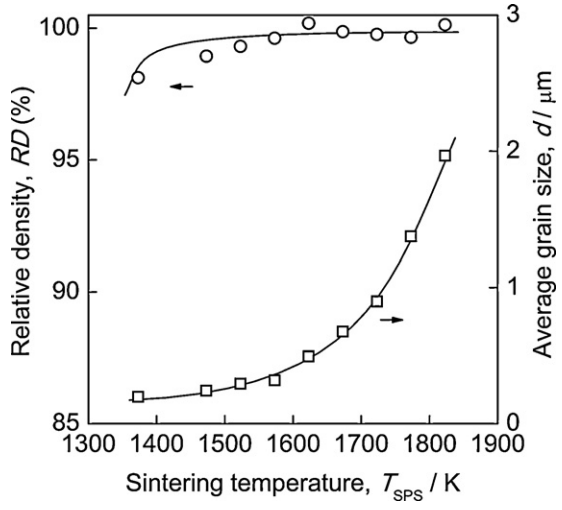

Fig. 4. Effect of sintering temperature on relative density and average grain size of Y_2O_3 bodies sintered by SPS.

Fig. 6 shows photographs of Y_2O_3 bodies sintered at 1573–1723 K before and after annealing at 1323 K for 21.6 ks in air. The text 30 mm underneath the Y_2O_3 bodies can be seen and all the specimens were dark gray (Fig. 6a–c). The gray color of the Y_2O_3 body sintered at 1573 K disappeared after annealing (Fig. 6d), while that of the Y_2O_3 bodies sintered at 1673 and 1723 (Fig. 6e and f) partially disappeared.

Fig. 7 shows transmittance spectra of Y_2O_3 bodies sintered at 1573 K before and after annealing at 1123–1423 K for 21.6 ks. With an increase in annealing temperature, the gray color disappeared gradually and transmittance increased over the entire wavelength range. The optimal annealing temperature was 1323 K (Fig. 7b). The ultraviolet absorption edge was blue-shifted from 308 to 256 nm with increasing annealing temperature from 1123 to 1223 K, and there was almost no change at higher annealing temperatures up to 1423 K.

Fig. 8 shows transmittance spectra of Y_2O_3 bodies sintered at 1473–1773 K after annealing at 1323 K for 21.6 ks in air (solid lines) and those calculated from the refractive index of an Y_2O_3 single crystal (dashed line). In-line transmittance (T) can be calculated by the Beer–Lambert law using the following equation[21]:

$$T = \frac{2n}{1+n^2} e^{-\alpha_t d}, \tag{3}$$

where n is the refractive index, α_t is the total absorption and d is the thickness of the specimen. Theoretical transmittance is depicted in Fig. 8 (dashed line) by substituting n of an Y_2O_3 single crystal[22] assuming $\alpha_t = 0$ in Eq. (3). n of the Y_2O_3 single crystal was 1.89 at $\lambda = 2000$ nm, where T was calculated as 82.6%. This value can be 100% of theoretical transmittance at $\lambda = 2000$ nm. The transmittance of the Y_2O_3 body increased significantly over the entire wavelength range after annealing. The Y_2O_3 body sintered at 1573 K showed the highest transmittance of 55.0% and 81.7% at $\lambda = 550$ and 2000 nm, respectively. The transmittance of the Y_2O_3 body sintered at 1573 K after annealing approached 99% of the calculated value in the infrared range (Fig. 8a). The sintering temperature used in this study (1573 K) for preparing highly transparent Y_2O_3 was significantly lower than that for pressureless sintering (above 1973 K),[5–8] hot

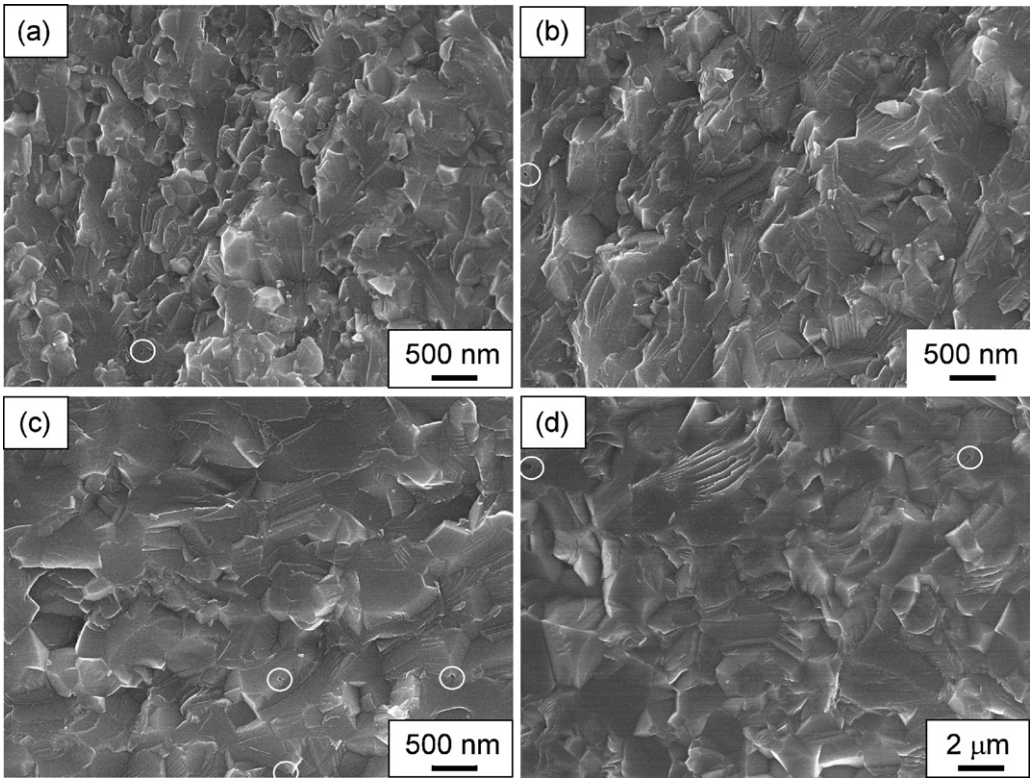

Fig. 5. FESEM images of fracture surfaces of Y_2O_3 bodies sintered at (a) 1473 K, (b) 1573 K, (c) 1673 K and (d) 1773 K. Open circles indicate pores.

pressing (1853 K)[10] and hot isostatically pressed two-step sintering (1773 K).[13] The highest transmittance at $\lambda = 700$ nm of the Y_2O_3 body in this study ($T = 68\%$) was higher than that of the Y_2O_3 body prepared by SPS using a low heating rate of 0.03 K s^{-1} ($T = 38\%$),[17] and was comparable to that of the Y_2O_3 body prepared using a high pressure of 300 MPa ($T = 68\%$).[18] It is known that an oxide vacancy readily forms in a vacuum during SPS, resulting in a gray color and degradation of transparency.[23] After annealing, the oxide vacancy can be eliminated, and thus the ultraviolet absorption edge was blue-shifted and the specimen became colorless.[24,25]

Fig. 9 shows the effect of sintering temperature on Vickers hardness (H_V) and the fracture toughness of the annealed Y_2O_3 bodies (Fig. 9a) and the relationship between H_V and grain size (Fig. 9b). H_V of the Y_2O_3 body sintered at 1373 K was 8.3 GPa and had a maximum value of 9.0 GPa at 1523 K, the value decreasing to 7.6 GPa with an increase in sintering temperature to 1823 K. The fracture toughness ranged from 1.5 to 1.0 MPa $m^{1/2}$ irrespective of sintering temperature, which was in accordance with the reported value.[13,26] H_V of the Y_2O_3 body sintered at 1523 K with an average grain size of about 0.29 μm was close to that of the Y_2O_3 body subjected to hot isostatic pressing with almost the same grain size.[13] Fig. 9b shows H_V as a function of the inverse square root of the grain size (d). H_V had a linear dependency with $d^{-1/2}$, obeying the Hall–Petch relation. Since the Y_2O_3 body sintered at 1373 K had a low density of 98%, it did not obey the relation. It is commonly observed that H_V increases with $d^{-1/2}$ in many ceramics, such as MgO,[27] $MgAl_2O_4$,[28] hydroxylapatite ($Ca_{10}(PO_4)_6(OH)_2$)[29] and Al_2O_3.[30,31] This can be attributed to the reducing free path for dislocation as the grain size decreases.[30] The Y_2O_3 bodies in the current study, with grains having diameters 0.24–1.97 μm, also followed this trend.

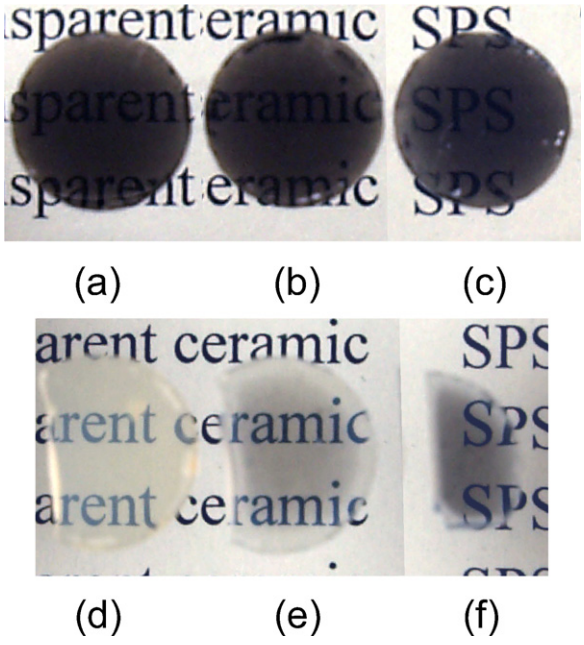

Fig. 6. Photograph of transparent Y_2O_3 bodies sintered at (a) 1573 K, (b) 1673 K and (c) 1723 K before annealing, and sintered at (d) 1573 K, (e) 1673 K and (f) 1723 K after annealing at 1323 K for 21.6 ks in air. The text is 30 mm underneath the specimens.

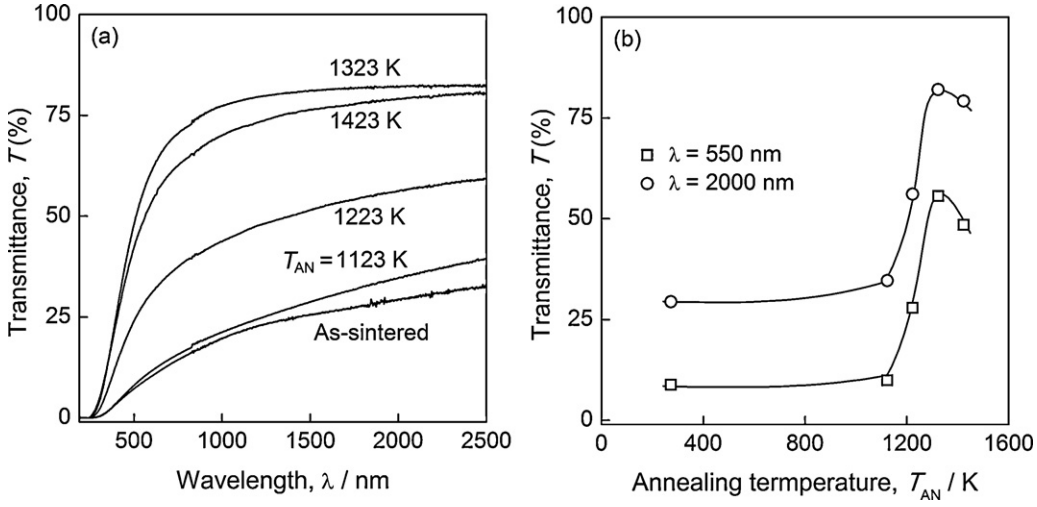

Fig. 7. (a) Transmittance spectra of Y_2O_3 bodies before and after annealing at 1123–1423 K for 21.6 ks using specimens sintered at 1573 K, and (b) transmittance at X = 550 and 2000 nm plotted as a function of annealing temperature.

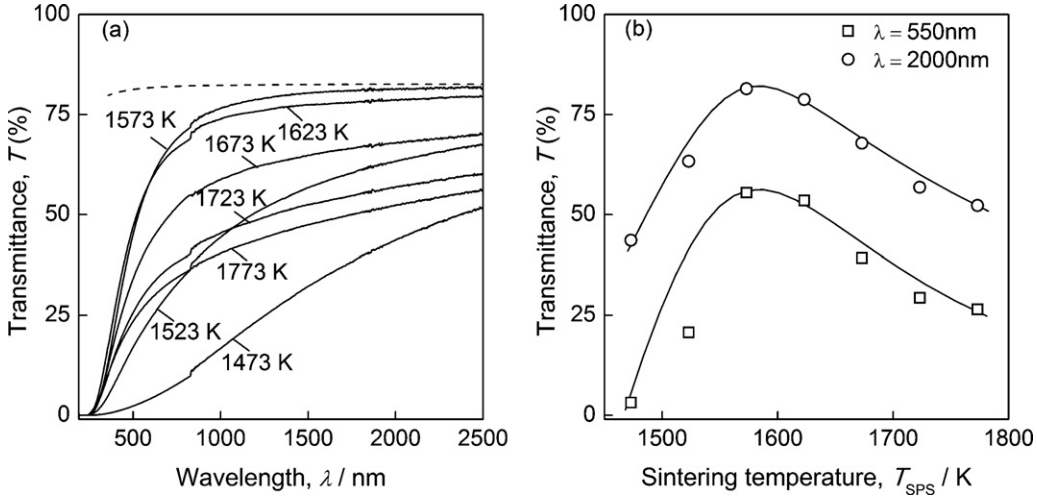

Fig. 8. (a) Transmittance spectra of Y_2O_3 bodies sintered at 1473–1773 K after annealing at 1323 K, and (b) transmittance at λ = 550 and 2000 nm plotted as a function of sintering temperature. The dashed line indicates transmittance calculated from the refractive index of Y_2O_3 single crystal.[22]

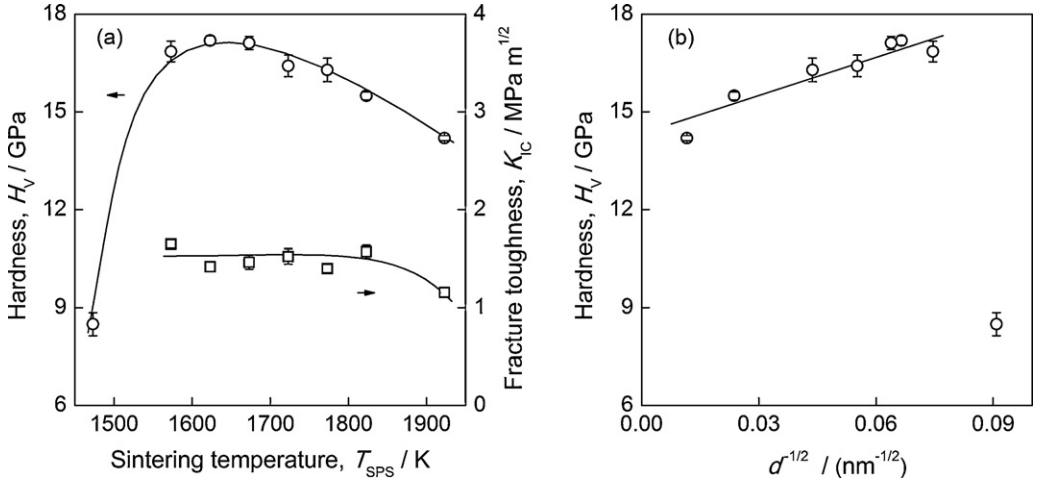

Fig. 9. (a) Effect of sintering temperature on Vickers hardness and fracture toughness of Y_2O_3 bodies annealed at 1323 K, and (b) Vickers hardness as a function of the inverse square root of the grain size (d).

4. Conclusions

Transparent Y_2O_3 bodies were fabricated by SPS at a low sintering temperature of 1573 K for 2.7 ks and annealing at 1323 K for 21.6 ks. Fully dense Y_2O_3 was obtained at the sintering temperatures 1473–1823 K. The average grain size was 0.24–0.32 μm at 1473–1573 K and steadily increased to 1.97 μm with an increase in temperature to 1823 K. After annealing at 1323 K, the gray color of the Y_2O_3 body sintered at 1573 K disappeared and the Y_2O_3 body showed the highest transmittance of 81.6% at 2000 nm (99% of a theoretical value). The Y_2O_3 body sintered at 1523 K had the highest hardness of 9.0 GPa.

Acknowledgements

This research was supported in part by the Research Fellowships of the Japan Society for the Promotion of Science for Young Scientists. It was also supported in part by the Global COE Program of Materials Integration, Tohoku University.

References

1. Kong J, Tang DY, Zhao B, Lu J, Udea K, Yagi H, et al. 9.2-W diode-end-pumped Yb:Y_2O_3 ceramic laser. *Appl Phys Let* 2005;**86**(16):161116.
2. Harris DC. *Materials for infrared windows and domes*. Washington: Society of Photo Optical; 1999.
3. Wei GC. Transparent ceramic lamp envelope materials. *J Phys D: Appl Phys* 2005;**38**(17):3057–65.
4. Wickersheim KA, Lefever RA. Infrared transmittance of crystalline yttrium oxide and related compounds. *J Opt Soc Am* 1961;**51**(10):1147–8.
5. Ikegami T, Ji JG, Mori T, Moriyoshi Y. Fabrication of transparent yttria ceramics by the low-temperature synthesis of yttrium hydroxide. *J Am Ceram Soc* 2002;**85**(7):1725–9.
6. Jin LL, Zhou GH, Shimai S, Zhang J, Wang SW. ZrO_2-doped Y_2O_3 transparent ceramics via slip casting and vacuum sintering. *J Eur Ceram Soc* 2010;**30**(10):2139–43.
7. Huang YH, Jiang DL, Zhang JX, Lin QL. Fabrication of transparent lanthanum-doped yttria ceramics by combination of two-step sintering and vacuum sintering. *J Am Ceram Soc* 2009;**92**(10):2883–7.
8. Zhang J, An LQ, Liu M, Shimai S, Wang SW. Sintering of Yb^{3+}:Y_2O_3 transparent ceramics in hydrogen atmosphere. *J Eur Ceram Soc* 2009;**29**(2):305–9.
9. Dutta SK, Gazza GE. Transparent Y_2O_3 by hot-pressing. *Mater Res Bull* 1969;**4**(11):791–6.
10. Podowitz SR, Gaumé R, Feigelson RS. Effect of europium concentration on densification of transparent Eu:Y_2O_3 scintillator ceramics using hot pressing. *J Am Ceram Soc* 2010;**93**(1):82–8.
11. Hergen E. Fabrication, optical transmittance, and hardness of IR-transparent ceramics made from nanophase yttria. *J Eur Ceram Soc* 2007;**27**(16):4711–7.
12. Mouzon J, Maitre A, Frisk L, Lehto N, Odén M. Fabrication of transparent yttria by HIP and the glass-encapsulation method. *J Eur Ceram Soc* 2009;**29**(2):311–6.
13. Serivalsatit K, Kokuoz B, Yazgan-Kokuoz B, Kennedy M, Ballato JM. Synthesis, processing, and properties of submicrometer-grained highly transparent yttria ceramics. *J Am Ceram Soc* 2010;**93**(5):1320–5.
14. Munir ZA, Quach DV, Ohyanagi M. Electric current activation of sintering: a review of the pulsed electric current sintering process. *J Am Ceram Soc* 2011;**94**(1):1–19.
15. Yoshida H, Morita K, Kim B-N, Hiraga K, Kodo M, Soga K, et al. Densification of nanocrystalline yttria by low temperature spark plasma sintering. *J Am Ceram Soc* 2008;**91**(5):1707–10.
16. Chaim R, Shlayer A, Estournes C. Densification of nanocrystalline Y_2O_3 ceramic powder by spark plasma sintering. *J Eur Ceram Soc* 2009;**29**(1):91–8.
17. Yoshida H, Morita K, Kim B-N, Hiraga K, Yamanaka K, Soga K, Yamamoto T. Low-temperature spark plasma sintering of yttria ceramics with ultrafine grain size. *J Am Ceram Soc* 2011;**94**(10):3301–7.
18. Zhang HB, Kim B-N, Morita K, Yoshida H, Hiraga K, Sakka Y. Fabrication of transparent yttria by high-pressure spark plasma sintering. *J Am Ceram Soc* 2011;**94**(10):3206–10.
19. Mendelson MI. Average grain size in polycrystalline ceramics. *J Am Ceram Soc* 1969;**52**(8):443–6.
20. Lawn BR, Fuller ER. Equilibrium penny-like cracks in indentation fracture. *J Mater Sci* 1975;**10**(12):2016–24.
21. Bernard-Granger G, Benameur N, Guizard C, Nygren M. Influence of graphite contamination on the optical properties of transparent spinel obtained by spark plasma sintering. *Scr Mater* 2009;**60**(3):164–7.
22. Nigara Y. Measurement of the optical constants of yttrium oxide. *Jpn J Appl Phys* 1968;**7**(4):404–8.
23. Wang C, Zhao Z. Transparent $MgAl_2O_4$ ceramic produced by spark plasma sintering. *Scr Mater* 2009;**61**(2):193–6.
24. Krell A, Klimke J, Hutzler T. Transparent compact ceramics: inherent physical issues. *Opt Mater* 2009;**31**(8):1144–50.
25. He XK, Liu MN, He YL, Zhao YQ, Xue DF. An optical spectroscopy study of defects in lithium tantalate single crystals. *Opt Commun* 2008;**281**(9):2531–4.
26. Albayrak IC, Basu S, Sakulich A, Yeheskel O, Barsoum M. Elastic and mechanical properties of polycrystalline transparent yttria as determined by indentation techniques. *J Am Ceram Soc* 2010;**93**(7):2028–34.
27. Nishida A, Shimamura T, Kohtoku Y. Effect of grain size on mechanical properties of high-purity polycrystalline magnesia. *J Ceram Soc Jpn* 1990;**98**(4):412–5.
28. Singh JP, Virkar AV, Shetty DK, Gordow RS. Strength-grain size relations in polycrystalline ceramics. *J Am Ceram Soc* 1979;**62**(3–4):179–83.
29. Wang JW, Shaw LL. Grain-size dependence of the hardness of submicrometer and nanometer hydroxyapatite. *J Am Ceram Soc* 2010;**93**(3):601–4.
30. Krell A, Blank P. Grain size dependence of hardness in dense submicrometer alumina. *J Am Ceram Soc* 1995;**78**(4):1118–20.
31. Rice RW. In: MacCrone RK, editor. *Treatise on materials science and technology*, vol. 11. New York: Academic Press; 1977. p. 199.